Available online at www.sciencedirect.com
ScienceDirect
Journal of Solid State Chemistry 180 (2007) 2061–2066
JOURNAL OF SOLID STATE CHEMISTRY
www.elsevier.com/locate/jssc

Synthesis and characterization of layered zinc hydroxychlorides

Hidekazu Tanaka[a,*], Akiko Fujioka[a], Aya Futoyu[a], Kazuhiko Kandori[b], Tatsuo Ishikawa[b]

[a]Department of Material Science, Faculty of Science and Engineering, Shimane University, 1060 Nishikawatsu, Matsue, Shimane 690-8504, Japan
[b]School of Chemistry, Osaka University of Education, 4-698-1 Asahigaoka, Kashiwara, Osaka 582-8582, Japan

Received 20 February 2007; received in revised form 29 April 2007; accepted 6 May 2007
Available online 13 May 2007

Abstract

Layered material of zinc hydroxychlorides ($Zn_5(OH)_8Cl_2 \cdot nH_2O$: ZHC), which is one of the basic zinc salts (BZS), was synthesized from ZnO nano-particles aged with aqueous $ZnCl_2$ solutions at different temperatures ranging from 6 to 140 °C for 48 h. X-ray diffraction (XRD) results indicated that the diffraction peaks of ZnO completely disappeared by aging at 6 °C and the ZHC peaks were developed. By increasing the aging temperature, crystallinity of the layered structure was improved. At 6 °C, the ZHC particles were thin hexagonal plate particles with sizes ranging from 1 to 3 μm. The particle size of ZHC was independent of aging temperature. The atomic Cl/Zn ratios of all the ZHC materials were almost 0.2 less than 0.4 of the theoretical ratio, indicating that the synthetic ZHC is Cl-deficient. It seemed that half of Cl atoms in the layer were replaced with HCO_3^- and/or OH^-. The specific surface areas of ZHC estimated from N_2 adsorption isotherms were ca. $10\,m^2\,g^{-1}$ and were independent of the aging temperature. However, the H_2O monolayer adsorption capacity per unit surface area (n_w) for all the samples was higher than that of ZnO particles, revealing the high affinity of ZHC to H_2O molecules. The n_w values were increased by reducing the crystallinity of ZHC. This enhancement of H_2O adsorption selectivity was thought to be related with less-crystallized parts of the particles.

Keywords: Zinc hydroxychloride; Layered material; Crystal structure; Gas adsorption; Adsorption selectivity

1. Introduction

Basic zinc salts of (BZS), e.g., zinc hydroxychlorides ($Zn_5(OH)_8Cl_2 \cdot H_2O$: simonkolleite or ZHC), zinc hydroxycarbonate ($Zn_5(CO_3)_2(OH)_6$: hydrozincite) and zinc hydroxysulfate ($Zn_4SO_4(OH)_6 \cdot nH_2O$), possess a layered structure [1]. Similar materials of layered double hydroxide ($[([M^{2+}_{1-x}M^{3+}_x(OH)_2]_x)A^{n-}_{n/x} \cdot mH_2O$, where M^{2+} and M^{3+} are divalent and trivalent metal ions, respectively: LDH) and hydroxy double salts ($[M^{2+}_{1-x}M'^{2+})(OH)_{3(1-y)}]^+ A^{n-}_{(1+3y)/n} \cdot mH_2O$, where M and M' are divalent metal ions such as Zn^{2+}: HDS) have been synthesized by many researchers and the materials have received attention in various applications such as catalysts, anion exchangers, adsorbents and so on [2–12]. However, synthesis and nature of BZS, particularly ZHC, have not been fully elucidated. Since the ZHC possesses the basal nano-sheets mainly composed of Zn(II) octahedron and tetrahedron and the Cl^- and H_2O molecules exist in the layer [1,13–16], the material is anticipated to be available for anion exchangers, adsorbents for gases, etc. However, to our knowledge, no study has been reported on the synthesis and nature of ZHC except for the study by Ishikawa et al. [17,18]. Recently, Ishikawa et al. [17,18] reported the synthesis of ZHC from aqueous $ZnCl_2$ solutions in the presence of Al(III) ions and indicated that the increasing atomic Al/Zn ratio in the starting solutions varied the crystal phases of the products as ZnO → ZnO + ZHC → ZHC → LDH. They further concluded that ZHC formation is effectively promoted by the addition of Al(III) ions. Nonetheless, Zn(II) atoms in the synthetic ZHC were partly replaced with Al(III). To elucidate the detailed information about formation condition and characterization of ZHC, synthesis of ZHC freed from Al(III) is required.

To clarify the formation, the condition of ZHC is also important in corrosion science. In industry, steels are often

*Corresponding author. Fax: +81 852 32 6823.
E-mail address: hidekazu@riko.shimane-u.ac.jp (H. Tanaka).

0022-4596/$ - see front matter © 2007 Elsevier Inc. All rights reserved.
doi:10.1016/j.jssc.2007.05.001

galvanized by different zinc alloys such as Zn–Al, Zn–Al–Mg, Zn–Al–Mg–Si to suppress the corrosion of steels. The high corrosion resistance was explained by the fact that the protecting property of zinc hydroxycarbonate formed in the solution containing Cl^- is related to the formation of a disordered layer structure producing adherent films [19]. Further, it has been reported that the zinc rusts contain various kinds of oxides, hydroxides and BZS depending on the exposure environment [1,19–24] and the ZHC is formed together with ZnO by exposing the Zn-coated steels the to industrial or marine atmosphere [20].

The aim of this study was to clarify the detailed nature of the ZHC, hence we tried to synthesize the ZHC by aging ZnO nano-particles in aqueous $ZnCl_2$ solutions at different temperatures of 6–140 °C and $ZnCl_2$ concentrations. The products thus obtained were characterized by X-ray diffraction (XRD), transmission electron microscopy (TEM), thermal analysis, inductively coupled plasma emission spectroscopy (ICP-AES), gas adsorption measurements and so on. The formation conditions and functions of ZHC are discussed in this article.

2. Experimental

2.1. Synthesis of ZnO particles

ZnO particles were synthesized by the following wet method. An aqueous solution (1.0 dm^3) of 50.0 mmol dm^{-3} $ZnCl_2$ was prepared and the pH of the solution was adjusted to 9.0 by adding a 28% NH_3 solution under stirring condition. The resultants were aged at 50 °C for 24 h in a sealed polyethylene terephtalate bottle without stirring. After aging, the resulting precipitates were filtered off, thoroughly washed with deionized-distilled water and finally dried at 50 °C in an air oven for 24 h.

2.2. Synthesis of ZHC particles

Preparation of ZHC particles was carried out in aqueous media as follows. The synthetic ZnO particles (16.0 mmol) were added into 50 ml of 0–2.0 mol dm^{-3} $ZnCl_2$ solutions in a sealed polypropyrene vessel or a stainless-steel autoclave and they were aged at 6–140 °C for 48 h without stirring. The precipitates generated were filtered off, washed with acetone and finally dried in vacuo at 50 °C for 24 h.

2.3. Characterization

The materials thus obtained were characterized by a variety of conventional techniques. Powder XRD patterns were taken on a Rigaku diffractometer with a Ni-filtered Cu$K\alpha$ radiation (30 kV, 16 mA). Particle morphology was observed by a JEOL TEM. Transmission IR spectra were recorded with a resolution of 4 cm^{-1} using a KBr method by a JASCO Fourier transform infrared (FTIR) spectrometer. Zn and Cl contents in the materials were respectively assayed by a Seiko ICP-AES and the Mohr method. The samples were dissolved in HNO_3 solutions. Thermal gravimetry (TG) and differential thermal analysis (DTA) curves were traced on a Rigaku thermoanalyzer at a heating rate of 10 °C min^{-1} under air stream. Specific surface area was obtained by fitting the BET equation to the N_2 adsorption isotherms measured by a Quntachrome volumetric apparatus at the boiling temperature of liquid nitrogen. Adsorption isotherms of H_2O were determined by a gravimetric technique at 25.0 °C. Prior to the adsorption measurements, the samples were treated at 100 °C under 10^{-5} Torr for 2 h.

3. Results and discussion

3.1. Influence of aging temperature and $ZnCl_2$ concentration on the formation of ZHC

The ZnO particles were aged in 2.0 mol dm^{-3} aqueous $ZnCl_2$ solutions at different temperatures of 6–140 °C for 48 h. Fig. 1 shows the XRD patterns of the products. Hereafter, $ZnCl_2$ concentration is abbreviated as $[Zn^{2+}]$. Pattern a is synthetic ZnO particles used as a raw material of ZHC (JCPDS no. 46-1451). At an aging temperature of 6 °C, the diffraction peaks due to ZnO completely vanish and new peaks mainly develop at $2\theta = 11.2°$, 22.5° and 46.0°, which can be ascribed to the ZHC (no. 7-195). These facts allow us to infer that the ZnO particles are hydrolyzed in $ZnCl_2$ solutions to recrystallize as ZHC by the following reactions:

$$ZnO + H_2O \rightarrow Zn^{2+} + 2OH^-,$$

$$5Zn^{2+} + 8OH^- + 2Cl^- + H_2O \rightarrow Zn_5(OH)_8Cl_2 \cdot H_2O.$$

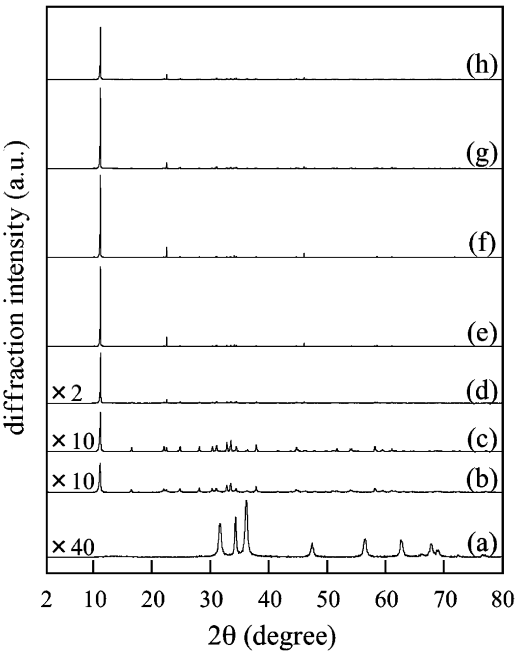

Fig. 1. XRD patterns of: (a) synthetic ZnO and (b–h) ZnO aged at $[Zn^{2+}] = 2.0$ mol dm^{-3} and different temperatures for 48 h. Aging temperature (°C), (b) 6, (c) 30, (d) 50, (e) 85, (f) 100, (g) 120 and (h) 140.

The diffraction intensity of ZHC, particularly the peak at $2\theta = 11.2°$, is increased by raising the aging temperature. Further, no remarkable differences in position and shape of the peaks are recognized. Fig. 2 plots the diffraction intensity of (110) and (003) peaks, which respectively correspond to the crystallinity of **a**- or **b**-direction and **c**-direction of the crystal, as a function of aging temperature. It is noteworthy that the diffraction intensity of the (003) peak dramatically increases as the aging temperature rises and is maximum at 120 °C. However, the intensity of the (110) peak is independent of the aging temperature. These facts prove that the increment of aging temperature improves the crystallinity of the layered structure. The interlayer **d** distance of the products estimated from the (003) diffraction peak ranges from 0.787 to 0.789 nm. On the other hand, the unit cell dimension **a** calculated from the (110) peak is 0.634–0.635 nm. The **d** and **a** values obtained are comparable to the literature values (**d** = 0.788 nm, **a** = 0.634 nm) [1]. Unfortunately, the crystallite size of the materials could not be determined because the values are beyond the evaluation limit of the crystallite size by the Scherrer equation (~300 nm).

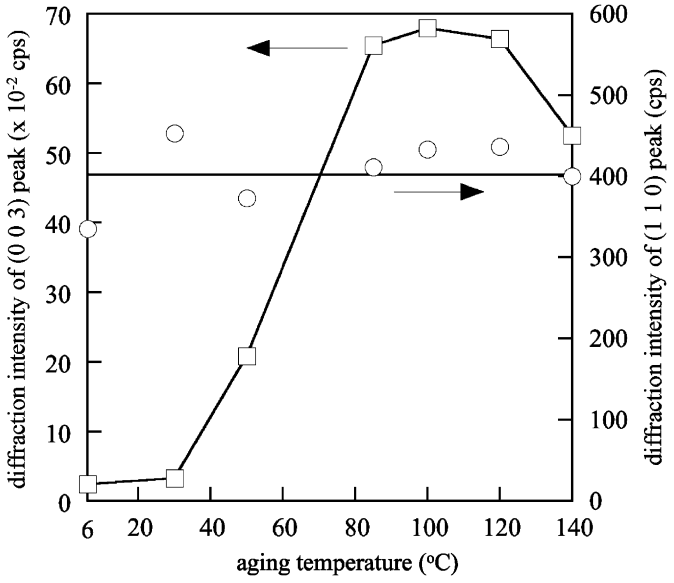

Fig. 2. Plots of diffraction intensity of: (□) (003), and (○) (110) peaks of ZHC as a function of aging temperature.

Fig. 3 displays the TEM pictures of the products formed at different aging temperatures and $[Zn^{2+}] = 2.0\,mol\,dm^{-3}$. The ZnO synthesized is fine irregular particles (picture a). At 6 °C, thin hexagonal plate particles with the sizes of 1–3 μm are seen and the fine ZnO particles completely disappear (picture b). As confirmed by XRD measurements, the ZHC is formed at the same aging temperature. It is, therefore, indicated that the hexagonal plate particles are identified as ZHC. No remarkable change in particle size of ZHC is recognized with an increase of aging temperature (pictures c and d).

The Zn and Cl contents of the products were almost constant at 9.32–9.54 and 1.80–1.93 mmol g^{-1} over the whole aging temperature, respectively. The theoretical Zn and Cl contents calculated from the chemical formula of ZHC ($Zn_5(OH)_8Cl_2 \cdot H_2O$) are 9.06 and 3.62 mmol g^{-1}, respectively. The Zn amount is close to the theoretical value, while the Cl content is almost half of the value, testifying that the materials are Cl-deficient. The starting $ZnCl_2$ solutions contain much larger amounts of Cl^- than the products. This suggests that the insufficient Cl source does not cause the Cl deficiency. To verify this, IR spectra were traced. Although the results are not shown here, the spectra of all the synthetic ZHC samples exhibited a weak stretching vibration C–O absorption band at 1410 cm^{-1} and the area intensity of this band was independent of the aging temperature. The ZHC crystals have a layered structure and the basal sheets were octahedrally and tetrahedrally coordinated with OH and Cl [1]. The Cl atoms are located in each top corner of the Zn(II) tetrahedron and the H_2O molecules are located between

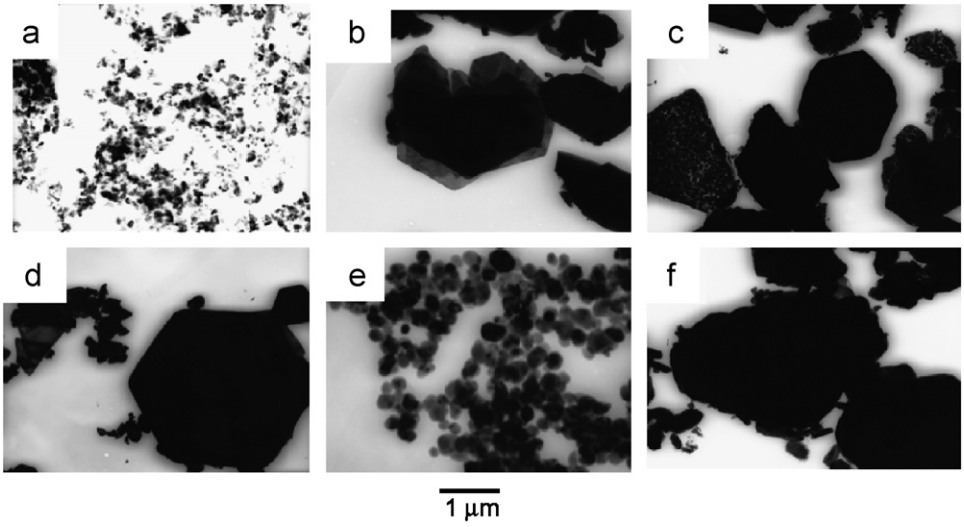

Fig. 3. TEM pictures of: (a) synthetic ZnO, (b–d) ZnO aged at $[Zn^{2+}] = 2.0\,mol\,dm^{-3}$ and elevated temperatures for 48 h and (e, f) ZnO aged at different $[Zn^{2+}]$ and 140 °C for 48 h. Aging temperature (°C), (b) 6, (c) 85, (d) 120. $[Zn^{2+}]$ (mol dm^{-3}), (e) 0.2 and (f) 0.5.

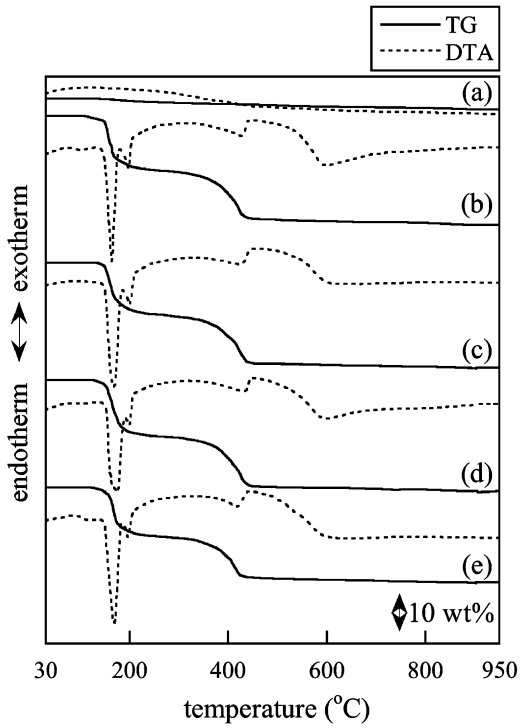

Fig. 4. TG-DTA curves in air of: (a) ZnO and (b–e) ZHC formed at $[Zn^{2+}] = 2.0\,mol\,dm^{-3}$ and different aging temperatures for 48 h. The solid and dotted lines represented TG and DTA curves, respectively. Aging temperature (°C), (b) 6, (c) 30, (d) 100, (e) 120.

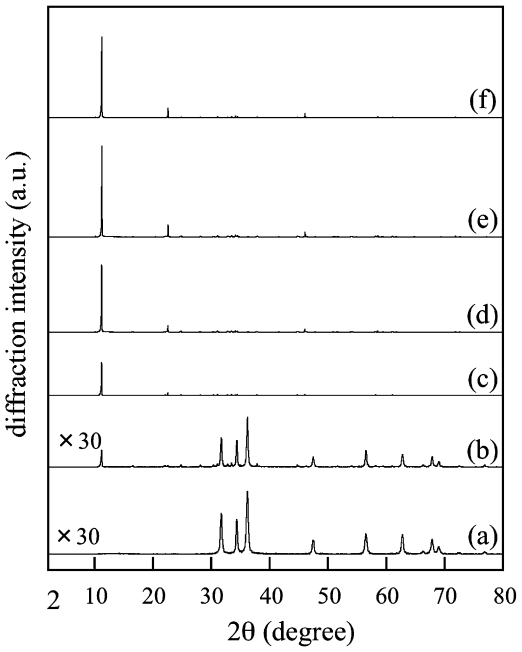

Fig. 5. XRD patterns of: (a) ZnO and (b–f) ZnO aged at different $[Zn^{2+}]$ and 140 °C for 48 h. $[Zn^{2+}]$ ($mol\,dm^{-3}$), (b) 0.2, (c) 0.5, (d) 1.0, (e) 1.5 and (f) 2.0.

the layers bound by weak hydrogen bonds of OH···Cl [1]. Moreover, Ghose has reported that the Cl atoms in the layer are replaced easily with carbonate ions [16]. Besides, Ishikawa et al. [17] recently indicated the replacement of Cl atoms in ZHC with HCO_3^-. It seems, therefore, that half of Cl atoms in the layer are replaced with HCO_3^- and/or OH^-, resulting in Cl deficiency in ZHC.

The thermal stability of ZHC was examined by TG and DTA. Fig. 4 shows the TG and DTA curves taken in an air stream for the products formed at various aging temperatures represented by solid and dotted lines, respectively. The TG curve a of ZnO shows a continuous mass loss from 200 to 950 °C with no DTA peak, in which the mass loss is mainly due to the removal of H_2O molecules strongly adsorbed and/or involved in the material. The TG curves of the materials obtained at 6 and 30 °C undergo a steep mass loss between 150 and 220 °C accompanying a strong endothermic DTA peak (curves b and c). As the aging temperature is raised, no remarkable change in mass loss value is recognized, while the endothermic peak slightly shifts to a higher temperature from 165 to 180 °C. As stated above, elevating the aging temperature increases the crystallinity of ZHC. It seems that the ZHC yielded at 6–30 °C contains poorly crystallized and hydrated parts such as an amorphous phase. Therefore, the mass loss would be due not only to removal of H_2O in the ZHC layer but also to dehydration of the amorphous phase, giving rise to a low-temperature shift of the DTA peak. Furthermore, the wide-range mass loss from 380 to 500 °C with an endothermic peak can be ascribed to the release of OH groups in the materials as H_2O molecules [17].

To verify the influence of $[Zn^{2+}]$ in the starting solution on the formation of ZHC, ZnO particles were aged at various $[Zn^{2+}]$ and 140 °C for 48 h. Fig. 5 shows the XRD patterns of the products. At $[Zn^{2+}] = 0.2\,mol\,dm^{-3}$, the diffraction peaks due to ZnO are faintly weakened and the weak peaks of ZHC appear. The ZnO peaks completely disappear at $[Zn^{2+}] = 0.5\,mol\,dm^{-3}$. The ZHC peaks are intensified with the increment of $[Zn^{2+}]$, showing a maximum at $[Zn^{2+}] = 1.5\,mol\,dm^{-3}$. The morphology of the particles was confirmed by TEM observation and the results are displayed in Figs. 3(e) and (f). When aged at $[Zn^{2+}] = 0.2\,mol\,dm^{-3}$, thin hexagonal plate ZHC particles with sizes ranging from 10 to 50 nm are observed in addition to the irregular ZnO particles (picture e). At $[Zn^{2+}] = 0.5\,mol\,dm^{-3}$, the ZHC particles grow and the irregular particles diminish, in accordance with the XRD results mentioned above (picture f). No remarkable difference in morphology of the ZHC particles yielded at $[Zn^{2+}] \geqslant 0.5\,mol\,dm^{-3}$ was recognized. The atomic Cl/Zn ratios of ZHC produced at $[Zn^{2+}] = 0.5$–$2.0\,mol\,dm^{-3}$ were ca. 0.2 less than 0.4 of the theoretical value, indicating that the materials are Cl-deficient. As suggested by the FTIR result, the Cl deficiency was caused by replacement of one-half of Cl in the layer with HCO_3^- and/or OH^-.

3.2. Adsorption of N_2 and H_2O

The adsorption property of the synthetic ZHC was examined by the adsorption of N_2 and H_2O. Fig. 6 shows the adsorption isotherms of N_2 on ZnO and ZHC

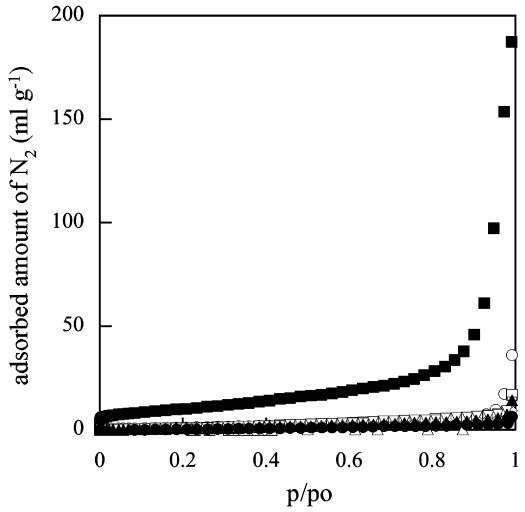

Fig. 6. N_2 adsorption isotherms on (■) ZnO and ZnO aged at $[Zn^{2+}] = 2.0\,mol\,dm^{-3}$ and different temperatures for 48 h. Aging temperature (°C), (○) 6, (□) 30, (△) 50, (◇) 85, (▽) 100, (●) 120 and (▲) 140.

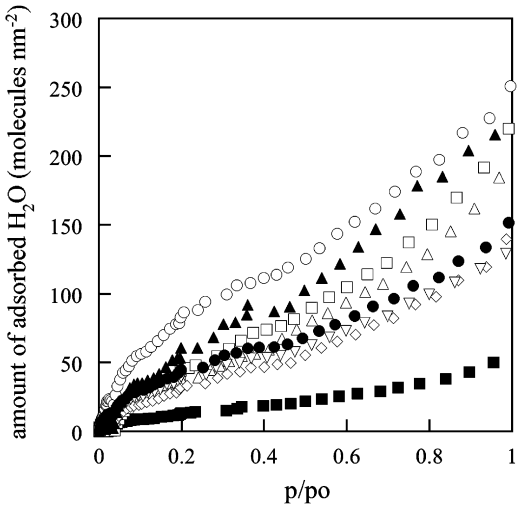

Fig. 7. H_2O adsorption isotherms on (■) ZnO and ZnO aged at $[Zn^{2+}] = 2.0\,mol\,dm^{-3}$ and different temperatures for 48 h. Aging temperature (°C), (○) 6, (□) 30, (△) 50, (◇) 85, (▽) 100, (●) 120 and (▲) 140.

synthesized at different aging temperatures of 6–140 °C for 48 h. The products at $[Zn^{2+}] = 2.0\,mol\,dm^{-3}$ were evacuated at 100 °C for 2 h prior to the adsorption measurements. The adsorption isotherm on ZnO represented by filled squares belongs to type II in the IUPAC classification. The specific surface area (S_n) of the material estimated from the BET equation was $39\,m^2\,g^{-1}$. The adsorbed amounts suddenly decrease with the formation of ZHC and the S_n values become ca. $10\,m^2\,g^{-1}$. The decrease of adsorbed amount and S_n is inferred to be due to the formation of larger ZHC particles than the ZnO ones as confirmed in Fig. 3. No micropores were ascertained by the *t*-plot analysis [25] for all the isotherms, meaning that the N_2 molecules cannot access the ZHC layer.

Fig. 7 compares the adsorption isotherms of H_2O on ZHC formed at various aging temperatures of 6–140 °C. The $[Zn^{2+}]$ and pretreatment temperature of the adsorption were the same as those of N_2 adsorption. Contrary to N_2 adsorption, the adsorbed amounts of H_2O on ZHC are larger than that on ZnO. This means that the materials exhibit a higher affinity to H_2O molecules than the N_2 ones. The adsorbed amount at $p/p_0 = 1.0$ is maximum at the aging temperature of 6 °C and decreases with increasing the aging temperature, while it slightly increases again at 140 °C. To clarify the difference among these isotherms, monolayer adsorption capacity of H_2O molecules per unit surface area (n_w) based on S_n is plotted against the aging temperature in Fig. 8. The n_w value (12.7) of ZnO is close to $9.3\,mol\,nm^{-2}$ of the theoretical n_w estimated using the $0.108\,nm^2$ as the cross-sectional area of a H_2O molecule, depicted by a dashed line. The n_w value is maximum at the aging temperature of 6 °C and is decreased with elevating the aging temperature. Fig. 8 plots the intensity of the (003) peak in XRD patterns by open circles as a function of the aging temperature. Clearly, we see that the increase of the diffraction intensity lowers the n_w value. This fact allows us

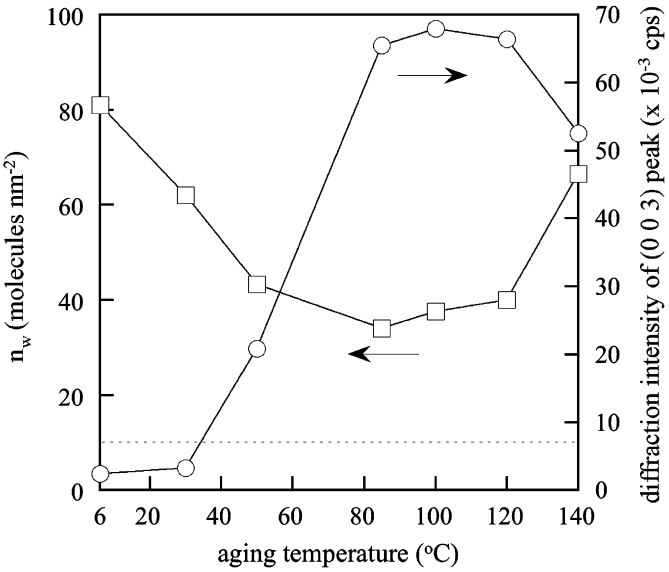

Fig. 8. Plots of (□) n_w and (○) diffraction intensity of (003) peak of ZHC against aging temperature.

to infer that the selective adsorption of H_2O molecules is dependent on the crystallinity of ZHC. The crystallinity of ZHC is improved with elevating the aging temperature. Hence, the enhancement of H_2O adsorption on the products formed at lower aging temperatures of 6–30 °C is thought to be due to the less crystallized and hydrated parts of the particles as confirmed by thermal analysis. It seems that the less-crystallized parts are dehydrated during the pretreatment of adsorption and the rehydration takes place by the H_2O adsorption. On the other hand, the H_2O adsorption selectivity falls with increasing crystallinity of ZHC because the amount of less crystallized and hydrated parts is reduced.

4. Conclusions

From the information presented in this publication, we can draw the following conclusions. Layered ZHC can be synthesized from nano-sized ZnO particles aged in aqueous $ZnCl_2$ solutions at 6–140 °C for 48 h. Elevating the aging temperature increases the crystallinity of ZHC. The ZHC was hexagonal plate particles of which the size was almost unchanged by raising the aging temperature. The synthetic ZHC was Cl-deficient, which would be caused by exchange of one-half of Cl in the layer with HCO_3^- and/or OH^-. The S_n values of ZHC were ca. $10\,m^2\,g^{-1}$ and were independent of the aging temperature. The n_w value of ZHC, that is, a measure of selective adsorption of H_2O, was higher than that of ZnO, showing the high affinity of ZHC to H_2O molecules. The n_w value was increased by decreasing the crystallinity of ZHC.

References

[1] I. Odnevall, C. Leygraf, Corrosion Sci 34 (1993) 1213.
[2] K. Chibwe, W. Jones, J. Chem. Soc. Chem. Commun. (1989) 926.
[3] M. Meyn, K. Beneke, G. lagaly, Inorg. Chem. 29 (1990) 5201.
[4] F. Cvani, F. Trifiri, A. Vaccari, Catal. Today 11 (1991) 173.
[5] M. Meyn, K. Beneke, G. lagaly, Inorg. Chem. 32 (1993) 1209.
[6] H. Motioka, H. Tagaya, M. Karasu, J. Kadokawa, K. Chiba, J. Mater. Res. 13 (1998) 848.
[7] J.-H. Choy, Y.-M. Kwon, K.-S. Han, S.-W. Song, S.H. Chang, Mater. Lett. 34 (1998) 356.
[8] T. Itoh, T. Shichi, T. Yui, K. Takagi, J. Colloid Interface Sci. 291 (2005) 218.
[9] C. Jaubertie, M.J. Holgado, M.S. San Roman, V. Rives, Chem. Mater. 18 (2006) 3114.
[10] Y. Wang, H. Gao, J. Colloid Interface Sci. 301 (2006) 19.
[11] J. Tronto, F. Leroux, M. Dubois, C. Taviot-Gueho, J.B. Valim, J. Phys. Chem. Solids 67 (2006) 978.
[12] M. Zimowska, A. Michalik-Zym, R. Janik, T. Machej, J. Gurgul, R.P. Socha, J. Podobinski, E.M. Serwicka, Catal. Today 119 (2007) 321.
[13] V.R. Allmann, Kristallografiya 126 (1968) 417.
[14] F.C. Hawthorne, E. Sokolova, Can. Mineral. 40 (2003) 939.
[15] M. Rajamathi, G. Thomas, P. Kamath, Proc. Ind. Acad. Sci. 113 (2001) 671.
[16] S. Ghose, Acta Crsystallogr. 18 (1964) 1051.
[17] T. Ishikawa, K. Matsumoto, K. Kandori, T. Nakayama, J. Solid State Chem. 179 (2006) 1110.
[18] T. Ishikawa, K. Matsumoto, K. Kandori, T. Nakayama, Colloids Surf. A 293 (2007) 135.
[19] W. Feitknecht, Chem. Ind. 36 (1959) 1102.
[20] A. Sakoda, N. Usuki, S. Wakano, M. Nishihara, Hyomen-Gijyutsu 40 (1989) 164.
[21] I. Odnevall, C. Leygraf, Corrosion Sci. 36 (1994) 1077.
[22] P. Quintana, L. Veleva, W. Cauich, P. Pomes, J.L. Pene, Appl. Surf. Sci. 99 (1996) 325.
[23] Q. Qui, C. Yan, Y. Wan, C. Cao, Corrosion Sci. 33 (2002) 2789.
[24] T. Ishikawa, K. Matsumoto, A. Yasukawa, K. Kandori, T. Nakayama, T. Tsubota, Corrosion Sci. 46 (2004) 329.
[25] B.C. Lippens, J.H. de Boer, J. Catal. 4 (1965) 319.